Appl Biochem Biotechnol (2007) 143:54–62
DOI 10.1007/s12010-007-8006-1

Accumulation of Silver(I) Ion and Diamine Silver Complex by *Aeromonas* SH10 biomass

Haoran Zhang · Qingbiao Li · Huixuan Wang · Daohua Sun · Yinghua Lu · Ning He

Received: 25 October 2006 / Accepted: 25 May 2007 /
Published online: 18 September 2007

Abstract The biomass of *Aeromonas* SH10 was proven to strongly absorb Ag^+ and $[Ag(NH_3)_2]^+$. The maximum uptake of $[Ag(NH_3)_2]^+$ was 0.23 g(Ag) g^{-1}(cell dry weight), higher than that of Ag^+. Fourier transform infrared spectroscopy spectra analysis indicated that some organic groups, such as amide and ionized carboxyl in the cell wall, played an important role in the process of biosorption. After SH10 cells were suspended in the aqueous solution of $[Ag(NH_3)_2]^+$ under 60°C for more than 12 h, $[Ag(NH_3)_2]^+$ was reduced to Ag(0), which was demonstrated by the characteristic absorbance peak of elemental silver nanoparticle in UV-VIS spectrum. Scanning electron microscopy and transmission electron microscopy observation showed that nanoparticles were formed on the cell wall after reduction. These particles were then confirmed to be elemental silver crystal by energy dispersive X-ray spectroscopy, X-ray diffraction, and UV-VIS analysis. This study demonstrated the potential use of *Aeromonas* SH10 in silver-containing wastewater treatment due to its high silver biosorption ability, and the potential application of bioreduction of $[Ag(NH_3)_2]^+$ in nanoparticle preparation technology.

Keywords Biosorption · Bioreduction · Silver ion · Diamine silver complex · Nanoparticle

Introduction

The technology of efficient silver recovery has been studied a lot for the treatment of silver-containing wastewater, for example, photographic processing waste. Traditional methods such as chemical absorption, oxidation-reduction, and electrolysis were limitedly used because of their technological and economical disadvantages [1–6]. As some microorganisms have been shown to be capable of adsorbing silver ions in the aqueous solution, many biosorption methods have been developed to treat silver-containing solution [7–9]. Previous

H. Zhang · Q. Li (✉) · H. Wang · D. Sun · Y. Lu · N. He
Department of Chemical and Biochemical Engineering, College of Chemistry and Chemical Engineering, The Key Lab for Chemical Biology of Fujian Province, Xiamen University, Xiamen 361005, People's Republic of China
e-mail: kelqb@jingxian.xmu.edu.cn

studies mainly focused on the removal silver ions at low concentration. The study of high silver concentration wastewater treatment was seldom reported. On the other hand, recent researches have shown that silver biosorption was not only the simple adsorption of silver ions onto the microbiological substances, and that under certain conditions, the reduction of silver ions could also occur. The fungi *Verticillium* [10] and *Fusarium oxysporum* [11] were found to be able to immobilize silver ions in aqueous solution and synthesize nano-sized silver particle through some enzyme-catalyzing reaction. *Pseudomonas stutzeri* AG259 was also shown to have the ability to grow in the aqueous solution of high Ag^+ concentration and accumulate silver crystals with the size up to 200 nm at the cell poles [12]. Despite many studies showing that the reduction of silver ions was enzyme-involved, there were some other reports showing that the formation of elemental silver could be a non-enzymatic process. Fu et al. [13] reported that *Lactobacillus* A09 biomass reduced Ag^+ ions through the interaction between Ag^+ and some organic groups on microbial cell wall. Further study on the binding of Ag^+ to A09 biomass showed that the hydrolysates of the polysaccharides from the cell wall were the main electron donor for Ag(I) reduction [14]. Besides Ag^+, $[Ag(NH_3)_2]^+$ was also used for the biosorption and bioreduction study. A previous study of our group found that *Corynebacterium* SH09 could strongly adsorb diamine silver complex and that 10–15 nm silver crystals were formed on the cell surface [15]. The formation of nano-sized silver particle on cell surface can be due to the organic structure of microbial cell wall, which might work as "scaffold" for growth of silver crystal and limit the size of the crystal.

In this paper, the biosorption and bioreduction of Ag^+ and $[Ag(NH_3)_2]^+$ by *Aeromonas* SH10 was investigated. Biosorption of Ag^+ and $[Ag(NH_3)_2]^+$ with high concentration by *Aeromonas* SH10 was studied for comparison, and the underlying mechanism was analyzed using Fourier transform infrared spectroscopy (FTIR). The formation of silver nanoparticles was observed by scanning electron microscopy (SEM) and transmission electron microscopy (TEM) and confirmed by energy dispersive X-ray spectroscopy (EDX), X-ray diffraction (XRD), and UV-VIS. The kinetics of bioreduction was studied through UV-VIS analysis.

Experimental

Aeromonas SH10 was isolated from sewage of Shanghang gold mine, Fujian, China. In the medium containing soya peptone of 1% (*w*/*w*) and beef extract of 0.5% (*w*/*w*), SH10 cells were grown at 30°C for 24 h and harvested by centrifugation (3,000×*g*, 10 min at room temperature). Cell pellets were washed three times by deionized water to eliminate the possible biosorption by the medium. SH10 biomass was dried and ground into fine particles before mixing with silver ion or diamine silver complex.

Diamine silver complex was prepared by adding aqueous ammonia into silver nitrate solution. Aqueous nitrate and ammonia were used to adjust the pH of silver nitrate and diamine silver complex solutions, respectively.

Dried SH10 biomass was mixed with aqueous solutions of silver nitrate or diamine silver complex at different pH values to obtain a concentration of 5 g/l (dried biomass) and then shaken at a rotation rate of 150 min^{-1} in the dark at 30°C. Biosorption reached the equilibrium after 30 min, and then cell pellets were collected by centrifugation (8,000 min^{-1}, 10 min at room temperature). The concentration of Ag (Ag^+ or $[Ag(NH_3)_2]^+$) in supernatant was measured by atomic absorption spectrophotometer (Pgeneral, China). The specific uptake of Ag was then calculated as follows:

$$Q\left(gg^{-1}\right) = V(C_i - C_r)/M_b$$

where V was the volume of sample solution (l), C_i and C_r were the initial and residual Ag concentration(g/l) in solution, respectively, and M_b was the weight of dried biomass (g).

The biomass was in contact with silver ions or silver diamine complex for at least 30 min before FTIR measurement to ensure that the absorption reached the equilibrium. Biomass before and after biosorption was dried under 60°C until the weight did not change. The FTIR spectra of SH10 biomass were measured by Nicolet Avatar 360 FTIR (Nicolet, USA). Samples for FTIR was dried at room temperature and mixed with KBr. The mixtures were ground and pressed to form thin wafers for FTIR analysis. Each sample was measured three times in the transmission mode at a resolution of 4 cm^{-1}. The spectra were smoothed after measurement. The number of smooth points is 13.500 cm^{-1}.

To further study the process of bioreduction, SH10 biomass was suspended at a concentration of 5 g/l in an aqueous solution containing 10 g/l Ag^+ or $[Ag(NH_3)_2]^+$ and kept in the dark to avoid the reduction of diamine silver complex by light. Time samples of suspension were taken and assayed by UNICAM UV-300 spectrophotometer (Thermo Spectronic, USA) at intervals. After bioreduction, SH10 biomass suspension samples were collected for the observation of SH10 cell morphology by LEO1530 SEM (LEO Electron Microscopy Ltd, Germany) and TECNAI F30 FEG TEM (Philips, The Netherlands). SH10 biomass containing nanoparticles after bioreduction was dried at room temperature and ground to powder for XRD analysis using X'Pert Pro X-ray Diffractometer (PANalytical B.V., The Netherlands).

Results and Discussion

Biosorption of Ag^+ and $[Ag(NH_3)_2]^+$

Although much effort was dedicated into the study of the binding of Ag^+ onto biomass [7, 16, 10–15], there were few reports on biosorption of $[Ag(NH_3)_2]^+$. As Ag^+ and $[Ag(NH_3)_2]^+$ represent different physiochemical property, the analysis of the uptake of these two ions will help to better study the mechanism of Ag-binding process.

Our preliminary experiments showed that the biosorption reached equilibrium in 20 min (data not shown), indicating that biosorption was a quick process. Therefore, the biomass was in contact with Ag^+ or $[Ag(NH_3)_2]^+$ for 30 min to ensure the equilibrium of biosorption. Figure 1 showed the effect of aqueous Ag concentration on biosorption of Ag^+ and $[Ag(NH_3)_2]^+$ at different pH values. The specific uptake of Ag^+ and $[Ag(NH_3)_2]^+$ at different pH value increased with aqueous Ag concentration. In the full range of Ag equilibrium concentration, the affinity series for binding was: $[Ag(NH_3)_2]^+ > Ag^+$ (pH=5) $> Ag^+$ (pH=2). The maximum uptake of Ag^+ at pH=5 was close to that of $[Ag(NH_3)_2]^+$ only when equilibrium Ag^+ concentration reached 7 g/l. The maximum uptake of $[Ag(NH_3)_2]^+$ by *Aeromonas* SH10 was 0.23 g/g, lower than the maximum uptake by *Corynebacterium* SH09 [15]. But compared with the results of other reports, Ag binding capability of SH10 was still relatively strong [7, 16]. The uptake of Ag^+ at pH=2 was much lower than at pH=5, which could be simply due to the competitive inhibition of silver ion accumulation by protons in the lower pH value solution. After biosorption of Ag^+, the pH value of the solution increased from 2 and 5 to 2.7 and 5.5, respectively. This result could be attributed to the ions exchange of H^+ with Na^+, K^+, and other metal ions initially bound in SH10 biomass.

It has been shown that Ag^+ was bound to the biomass through ion exchange and coordination [16]. Functional groups in the cell wall cannot only absorb Ag^+ via electrostatic interaction, but also form complex with Ag^+. Compared with Ag^+, $[Ag(NH_3)_2]^+$ was subject

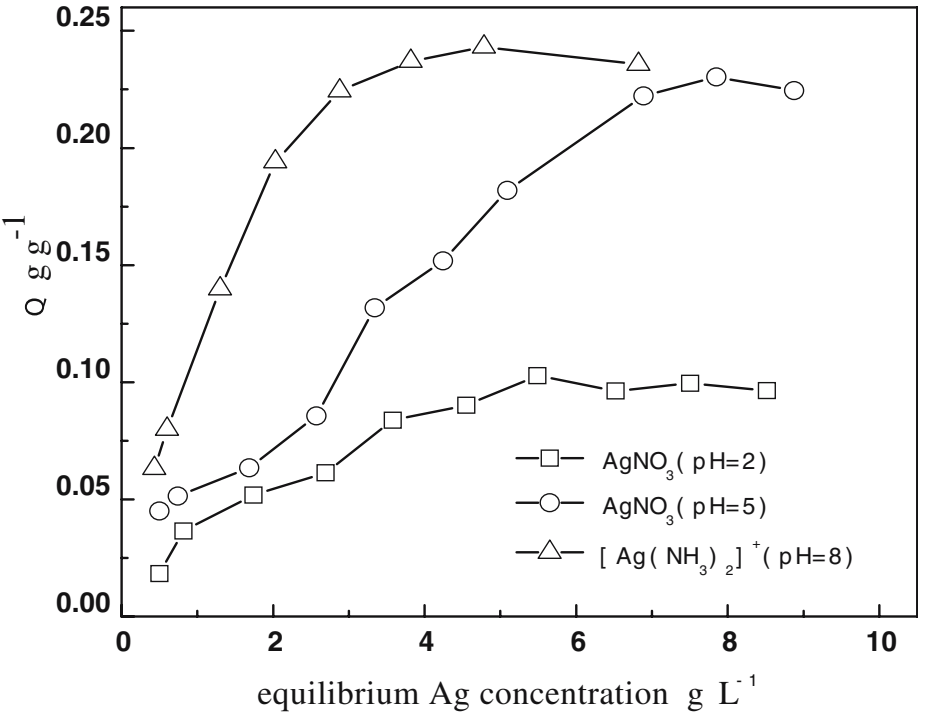

Fig. 1 Effect of equilibrium $[Ag(NH_3)_2]^+$ and Ag^+ concentration on uptake by *Aeromonas* SH10 (*Aeromonas* SH10 biomass concentration 5 g/l, temperature 30°C, contact time 6 h at 150 min^{-1})

to greater steric hindrance in the process of binding onto the SH10 biomass. Besides, $[Ag(NH_3)_2]^+$ is already a complex, and thus, Ag(I) in $[Ag(NH_3)_2]^+$ has a lower affinity to the organic group on the cell wall than free Ag^+. Surprisingly, the uptake of $[Ag(NH_3)_2]^+$ by SH10 was higher than that of Ag^+, indicating that $[Ag(NH_3)_2]^+$ was more easily immobilized. The reasons for this include: (1) in basic $[Ag(NH_3)_2]^+$ solution, the competitive inhibition of $[Ag(NH_3)_2]^+$ accumulation by H^+ was reduced; (2) in basic solution, more negative-charged groups on the surface of biomass were activated as binding sites.

Group Changes After Biosorption

Figure 2 presented the FTIR absorption spectra of *Aeromonas* strain SH10 cells before and after biosorption. Curve (a), (b) and (c) are the spectra before biosorption after the binding of Ag^+ and $[Ag(NH_3)_2]^+$, respectively. The absorbance band at 1654 cm^{-1} in curve (a) was associated with the carbonyl stretch vibration in the amide linkages of peptide chains of biomass. The band at 1,544 cm^{-1} was identified as another amide band, which arose due to the combination of N–H bending mode and C–N stretch vibration mode. After biosorption of Ag^+, these two bands shifted to 1,649 cm^{-1} and 1,538 cm^{-1}, respectively, as shown in curve (b), which demonstrated that amide linkages, specifically C=O and C–N, were bound with Ag^+ in the process of biosorption and changed their vibrational frequencies. These two bands in Curve (c) moved to 1,649 cm^{-1} and 1,536 cm^{-1}, showing the similar interaction between amide and $[Ag(NH_3)_2]^+$. The band at 1,396 cm^{-1} was attributed to asymmetrical

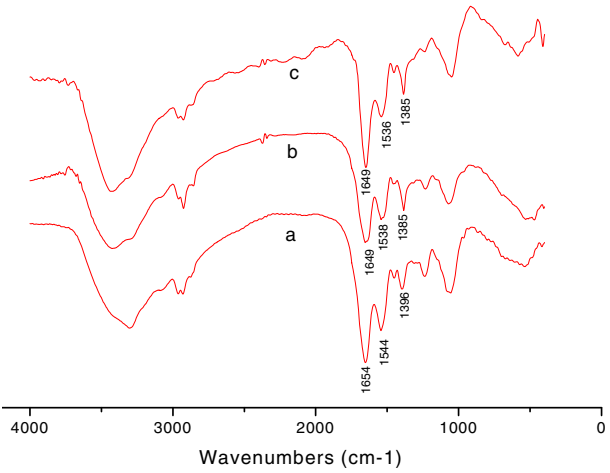

Fig. 2 FTIR absorption spectra of *Aeromonas* strain SH10 biomass before biosorption (***a***), after biosorption of Ag^+ (***b***), and $[Ag(NH_3)_2]^+$ (***c***)

stretch vibration of the ionized carboxyl of some amino acid residues of peptide chains. After biosorption of Ag^+ and $[Ag(NH_3)_2]^+$, the band shifted to 1,385 cm^{-1}, indicating that ionized carboxyl was combined with Ag^+ or $[Ag(NH_3)_2]^+$. Our previous finding indicated that the intensity of ionized carboxyl band increased dramatically after the bioreduction of $[Ag(NH_3)_2]^+$, whereas only the binding of $[Ag(NH_3)_2]^+$ cannot cause such a change [15]. This paper also showed that biosorption of $[Ag(NH_3)_2]^+$ promoted the shift of ionized carboxyl band in FTIR spectrum, but hardly changed its intensity.

Observation and Confirmation of the Formation of Silver Nanoparticles

Transmission electron micrographs in Fig. 3a displayed the morphology of SH10 cell after 72-h bioreduction of $[Ag(NH_3)_2]^+$ at 60°C. A large quantity of black particles was found on the cell surface. The distribution of the diameters of the particles was from several nanometers to around 20 nm, as shown in Fig. 3b. No such particles were observed when Ag^+ was used (data not shown). To further study these nanoparticles, EDX was used to analyze the elemental composition of our samples after bioreduction. EDX spectrum of SH10 biomass after bioreduction of $[Ag(NH_3)_2]^+$ showed the existence of abundant silver element Fig. 3c. Element P, O, and S in the EDX spectrum should come from the biomass of SH10. As no other metal element was found by EDX, it can be ruled out that the nanoparticles were composed of the element other than silver. Subsequent XRD analysis indicated that the nanoparticles in SH10 biomass were the crystal of Ag(0). As shown in Fig. 3d, four major peaks in bioreduction sample's XRD pattern corresponded to the characteristic diffraction peaks of elemental Ag, respectively. These results, together with the UV spectra analysis presented below, confirmed that nanosilver particles were formed after the bioreduction of $[Ag(NH_3)_2]^+$ by SH10 biomass.

Silver Nanoparticle Formation Kinetics

UV-VIS absorption spectra had been proven sensitive in detecting the formation of elemental silver nanoparticles. The absorption peak at around 400 nm is the characteristic surface plasmon absorption peak of silver nanoparticles and the position of the absorption peak depends on the particle size and shape [17, 18].

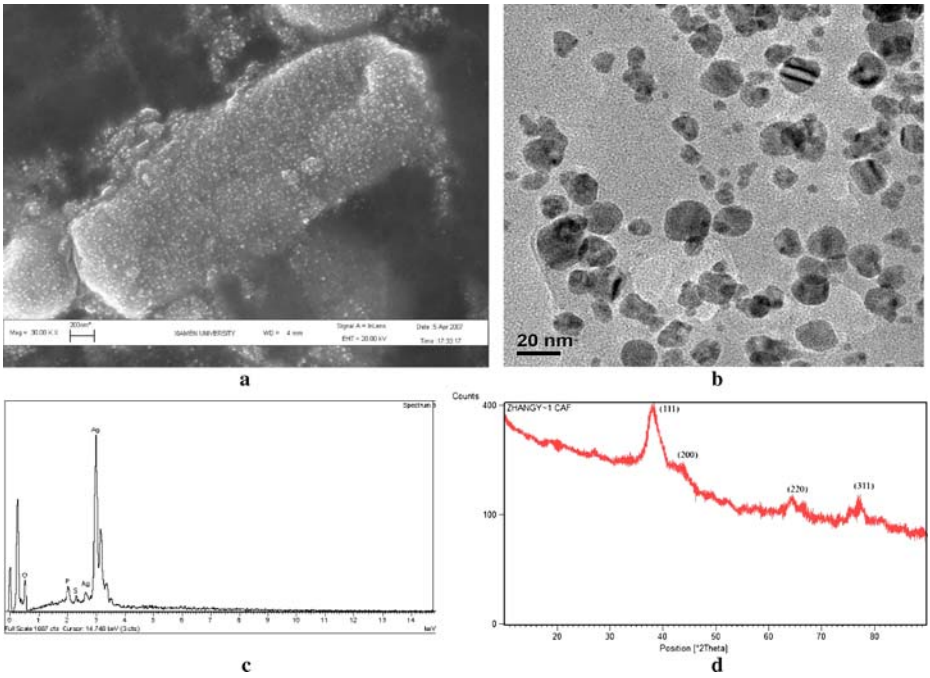

Fig. 3 **a** SEM micrographs, **b** TEM micrographs, **c** EDX spectrum, and **d** XRD spectrum of SH10 cell after bioreduction of $[Ag(NH_3)_2]^+$ at 60°C. The initial Ag and biomass concentrations were 10 g/l and 5 g/l, respectively. Contact time was 72 h. **a** After bioreduction, numerous particles were formed on the surface of SH10 biomass. **b** The size of these particles ranges from several nm to around 20 nm. **c** EDX spectrum indicated that the particle should contain Ag element. **d** XRD pattern investigation confirmed that these nanoparticles were elemental Ag crystal. Labeled peaks corresponded to the characteristic diffraction peaks of elemental Ag

Under the experimental conditions given above, no characteristic plasmon absorption peak was found when SH10 biomass was mixed with Ag^+ solution. However, the peak could be easily observed in the case of $[Ag(NH_3)_2]^+$.This is because the thermodynamic condition favors the reduction of $[Ag(NH_3)_2]^+$. In fact, in acid solution, the redox potential of nitrate ion is higher than that of Ag^+. Therefore, it is nitrate ion, instead of Ag^+, that is reduced when oxidation-reduction reaction occurs. In basic $[Ag(NH_3)_2]^+$ solution, no nitrate ion is present, and $[Ag(NH_3)_2]^+$ will be reduced by the reducing groups of SH10 biomass. Esumi et al. [19] also found that basic solution is necessary for the reduction of silver ion by their reducing agent sugar ball.

The preliminary study showed that the appearance of the characteristic Ag(0) peak was earlier when higher temperature was used, which indicated that temperature greatly influenced bioreduction process of $[Ag(NH_3)_2]^+$. Among the temperature range used in this study (20–60°C) 60°C was the most favorable temperature for bioreduction. Therefore, 60°C was chosen for silver nanoparticle formation kinetics study. Figure 3a presented the UV-VIS absorption spectra of silver nanoparticles formed during the process of the bioreduction of $[Ag(NH_3)_2]^+$ by SH10 at 60°C. After 0.5 day, a characteristic absorption peak maximum at 430 nm became evident, indicating the formation of silver nanoparticles. As shown in Fig. 3b, the absorbance of the peak increased with time, which indicated the increasing reduction of $[Ag(NH_3)_2]^+$ to Ag^0. The reduction rate was almost constant before day 5, and

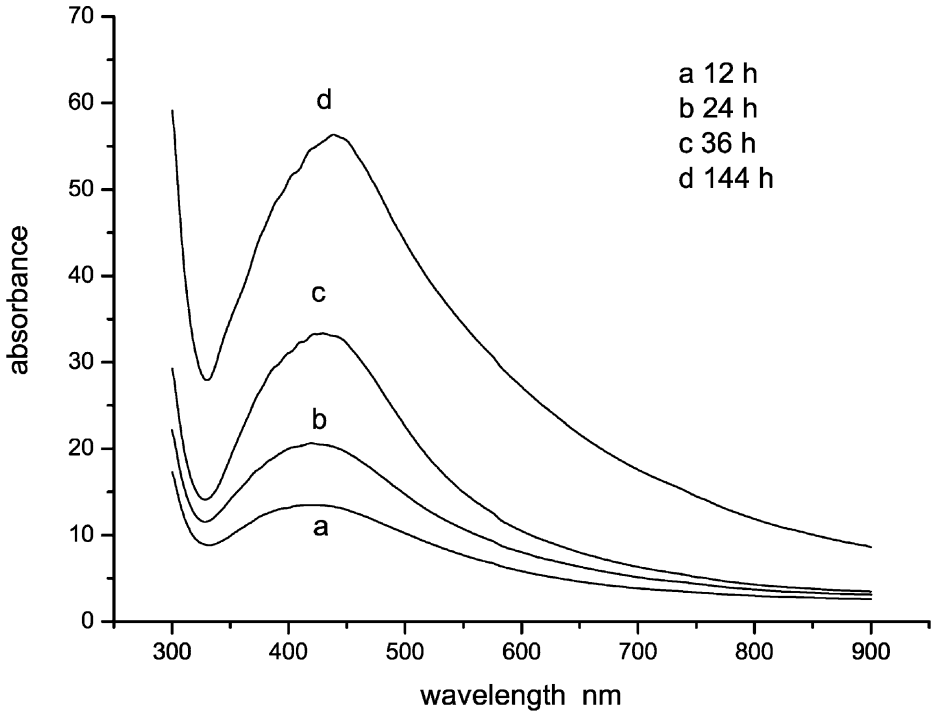
a 12 h
b 24 h
c 36 h
d 144 h
absorbance
wavelength nm
a
b
c
d

a

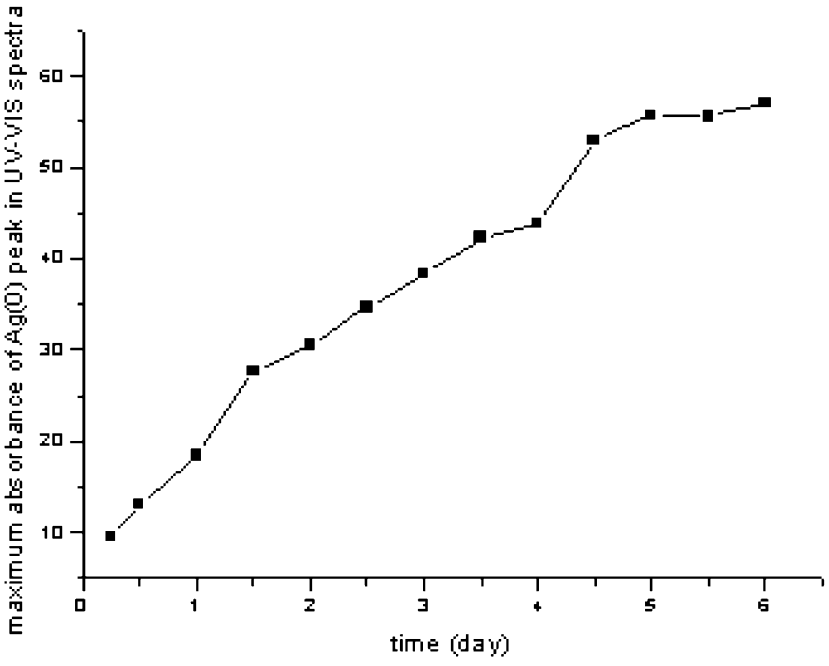
maximum absorbance of Ag(0) peak in UV-VIS spectra
time (day)

b

then the maximum absorbance ceased to increase after day 5, showing that the reduction reaction was ended.

It should be noticed that the characteristic absorption peak shifted a little towards longer wavelength as time increased. As the larger particle can cause the shift of absorption peak towards a longer wavelength, this result suggested that the silver nanoparticles grew with time. It has been shown that synthesized silver nanoparticles grew with time [20, 15], which was in agreement with our finding (Fig. 4).

Based on our findings, the process of biosorption and subsequent bioreduction of $[Ag(NH_3)_2]^+$ could be hypothesized as following. $[Ag(NH_3)_2]^+$ was first trapped on the cell wall through biosorption. Such groups, such as ionized carboxyl of amino acid residues and amide of peptide chains, provided the active sites for binding. Then, some reducing groups in the biomass, which might include aldehyde [15], ketone [15], and some reducing hydrolysates of polysaccharides [14], reduced $[Ag(NH_3)_2]^+$ to Ag(0) nuclei. These nuclei then grew into Ag(0) clusters or crystals as biosorption and bioreduction proceeded. As the surface morphology and organic structure of SH10 cells hindered the migration and aggregation of these crystals along the cell surface, the further growth of these crystals were limited and nano-sized particles were formed. It can be concluded that the reduction of $[Ag(NH_3)_2]^+$ by SH10 was a non-enzymatic process because enzymes in the SH10 biomass were inactivated under the experimental conditions of this study. Compared with other studies on silver bioreduction [10, 12, 13, 14], this non-enzymatic bioreduction process showed advantages in the following aspects. (1) The bioreduction is easy to achieve, and the process is easy to be scaled up. (2) A large quantity of silver nanopartilce can be produced under our experimental condition. (3) No enzyme is involved, so there is no need to maintain the reaction solution in special conditions to keep enzyme activity. (4) As the growth of the microorganism was to be decoupled with biosorption and bioreduction process, high concentration $[Ag(NH_3)_2]^+$ or Ag^+ solution can be treated regardless of the toxicity of these ions to microbial cell.

Conclusion

In this paper, *Aeromonas* strain SH10 was shown to be capable of strongly binding Ag^+ and $[Ag(NH_3)_2]^+$. FTIR spectra analysis indicated that ionized carboxyl of amino acid residues and amide of peptide chains in the biomass were involved in biosorption. Under certain conditions, SH10 could also reduce immobilized $[Ag(NH_3)_2]^+$ to elemental Ag(0), and nanoparticles of silver crystal was formed. We have studied the biosorption and bioreduction of $[Ag(NH_3)_2]^+$ by a gold-mine-isolated bacterium *Corynebacterium* SH09 [15]. The results of this paper demonstrate that SH10 biomass also has a strong accumulation ability of $[Ag(NH_3)_2]^+$ and that SH10 can be used as adsorbent for Ag remediation from silver-containing wastewater. Our future study will focus on (1) the analysis the biosorption and bioreduction ability of plant cells and other microorganism cell, finding whether $[Ag(NH_3)_2]^+$ biosorption and bioreduction ability are exclusively possessed by certain bacterium strains, (2) the separation of silver nanoparticle from microorganism biomass and the prevention of the separated nanoparticles from aggregation.

◀ **Fig. 4** UV-VIS absorption spectra (**a**) and formation kinetics (**b**) of silver nanoparticles after bioreduction by *Aeromonas* strain SH10 at 60°C. The initial concentration of $[Ag(NH_3)_2]^+$ and biomass were 10 and 5 g/l, respectively

This study showed the high silver accumulation ability of *Aeromonas* SH10, which indicated the potential application of this technology in silver-containing wastewater treatment. Moreover, it was found that the bioreduction of $[Ag(NH_3)_2]^+$ by *Aeromonas* SH10 biomass produced stable nano-sized Ag(0) particles, which suggested a new method for metal nanoparticle preparation.

Acknowledgment This work is part of the project (20376076) supported by National Natural Science Foundation of China. The authors thank Analysis and Testing Center of Xiamen University for the help of SEM and TEM analysis in this study.

References

1. Hilmi, A., Luong, J., & Nguyen, A. (1999). Utilization of TiO2 deposited on glass plates for removal of metals from aqueous wastes. *Chemosphere, 38*, 865–874.
2. Adani, K. G., Barley, R. W., & Pascoe, R. D. (2005). Silver recovery from synthetic photographic and medical X-ray process effluents using activated carbon. *Mineral Engineering, 18*, 1269–1276.
3. Othman, N., Mat, H., & Goto, M. (2006). Separation of silver from photographic wastes by emulsion liquid membrane system. *Journal of Membrane Science, 282*, 171–177.
4. Chen, J. P., & Lim, L. L. (2002). Key factors in chemical reduction by hydrazine for recovery of precious metals. *Chemosphere, 49*, 363–370.
5. Pollet, B., Lorimer, J. P., Phull, S. S., & Hihn, J. Y. (2000). Sonoelectrochemical recovery of silver from photographic processing solutions. *Ultrasonics Sonochemistry, 7*, 69–76.
6. Ajiwe, V. I. E., & Anyadiegwu, I. E. (2000). Recovery of silver from industrial wastes, cassava solution effects. *Separation and Purification Technology, 18*, 89–92.
7. Fourest, E., Canal, C., & Roux, J. (1994). Improvement of heavy metal biosorption by mycelial dead biomasses (*Rhizopus arrhizus*, *Mucor miehei* and *Penicillium chrysogenum*): pH control and cationic activation. *FEMS Microbiology Reviews, 14*, 325–332.
8. Pethkar, A. V., & Paknikar, K. M. (2003). Thiosulfate biodegradation–silver biosorption process for the treatment of photofilm processing wastewater. *Process Biochemistry, 38*, 855–860.
9. Simmons, P., & Singleton, I. (1996). A method to increase silver biosorption by an industrial strain of Saccharomyces cerevisiae. *Applied Microbiology and Biotechnology, 45*, 278–285.
10. Mukherjee, P., Ahmad, A., Mandal, D., Senapati, S., Sainkar, S. R., Khan, M. I., et al. (2001). Fungus-Mediated Synthesis of Silver Nanoparticles and Their Immobilization in the Mycelial Matrix: A Novel Biological Approach to Nanoparticle Synthesis. *Nano Letters, 1*, 515–519.
11. Ahmad, A., Mukherjee, P., Senapati, S., Mandal, D., Khan, M. I., Kumar, R., et al. (2003). Extracellular biosynthesis of silver nanoparticles using the fungus *Fusarium oxysporum*. *Colloids and Surfaces B, 28,* 313–318.
12. Klaus, T., Joerger, R., Olsson, E., & Granqvist, C. G. (1999). Silver-based crystalline nanoparticles, microbially fabricated. *Proceedings of the National Academy of Sciences of the United States of America, 96*, 13611–13614.
13. Fu, J., Liu, Y., Gu, P., Tang, D., Lin, Z., Yao, B., et al. (2000). Spectroscopic characterization on the biosorption and bioreduction of Ag(1) by Lactobacillus sp. A09. *Acta Physico-Chimica Sinica, 16*, 779–782.
14. Lin, Z., Zhou, C., Wu, J., Zhou, J., & Wang, L. (2005). A further insight into the mechanism of Ag+ biosorption by Lactobacillus sp. strain A09, *Spectrochimica Acta, 61*, 1195–1200.
15. Zhang, H., Li, Q., Lu, Y., Sun, D., Lin, X., Deng, X., et al. (2005). Biosorption and bioreduction of diamine silver complex by *Corynebacterium*. *Journal of Chemical Technology and Biothechnology, 80*, 285–290.
16. Tobin, J. M., Cooper, D. G., & Neufeld, R. J. (1984). Uptake of Metal Ions by *Rhizopus arrhizus* Biomass. *Applied and Environmental Microbiology, 47*, 821–824.
17. Kapoor, S. (1998). Preparation, Characterization, and Surface Modification of Silver Particles. *Langmuir, 14*, 1021–1025.
18. Zhu, J. J., Liu, S. W., Palchik, O., Koltypin, Y., & Gedanken, A. (2000). Shape-Controlled Synthesis of Silver Nanoparticles by Pulse Sonoelectrochemical Methods. *Langmuir, 16*, 6396–6399.
19. Esumi, K., Hosoya, T., Suzuki, A., & Torigoe, K. (2000). Formation of Gold and Silver Nanoparticles in Aqueous Solution of Sugar-Persubstituted Poly(amidoamine) Dendrimers. *Journal of Colloid and Interface Science, 226*, 346–352.
20. Lee, M. H., Oh, S. G., Suh, K. D., Kim, D. G., & Sohn, D. (2002). Preparation of silver nanoparticles in hexagonal phase formed by nonionic Triton X-100 surfactant. *Colloids and Surfaces A, 210*, 49–60.